JGS
Journal of the Geological Society

Research article

Published online November 22, 2016 https://doi.org/10.1144/jgs2016-014 | Vol. 174 | 2017 | pp. 289–300

Middle Jurassic shear zones at Cap de Creus (eastern Pyrenees, Spain): a record of pre-drift extension of the Piemonte–Ligurian Ocean?

Reinoud L. M. Vissers[1]*, Douwe J. J. van Hinsbergen[1], Camilla M. Wilkinson[2] & Morgan Ganerød[2]

[1] Department of Earth Sciences, University of Utrecht, Budapestlaan 4, 3584 CD Utrecht, Netherlands
[2] Geological Survey of Norway, Centre for Geodynamics, Leiv Eirikssons vei 39, 7491 Trondheim, Norway
* Correspondence: r.l.m.vissers@uu.nl

Abstract: The Cap de Creus peninsula in NE Spain consists of greenschist- to amphibolite-facies metasediments and granitoid bodies of the Variscan Axial Zone of the Pyrenees, overprinted in the north by anastomosed greenschist-facies shear zones. Current tectonic interpretations ascribe these shear zones to the waning stages of the Variscan orogeny. We present muscovite $^{40}Ar/^{39}Ar$ data from the shear zones, yielding Middle Jurassic ages between 159.33 ± 0.43 and 175.18 ± 1.10 Ma and one Tertiary age of 58.57 ± 0.55 Ma. We suggest that the present-day structure at Cap de Creus resulted from Variscan deformation and HT–LP metamorphism, followed during the Jurassic by crustal stretching and development of ductile normal faults reflecting pre-drift continental extension related to opening of the Piemonte–Ligurian basin east of Iberia. Tilting during Alpine convergence caused steepening in the northern part of the penisula, with the ductile normal faults rotated to their present orientations appearing as dextral reverse shear zones. The shear zone yielding a Tertiary age could reflect either an Alpine structure or reactivation of an earlier, presumably Jurassic shear zone. The Cap de Creus structure may thus represent a continental margin that has undergone ductile stretching equivalent to the now-buried west Iberian or Newfoundland margin.

Received 29 January 2016; **revised** 25 August 2016; **accepted** 18 September 2016

The Cap de Creus area in NE Spain is famous among structural geologists for the excellent exposure of a system of anastomosed greenschist-facies shear zones (Carreras & Santanach 1973; Druguet 1997; Carreras 2001, and references therein). The Cap de Creus peninsula forms the easternmost part of the Pyrenees (Fig. 1) and is made up of Variscan greenschist- to amphibolite-facies metasediments and granitoid bodies that belong to the Pyrenean Axial Zone (Zwart 1979). Local migmatites and one of the granodiorite bodies in the area have yielded 299 – 291 Ma U/Pb zircon ages, which demonstrate a Variscan age of the LP–HT metamorphism and granodiorite intrusion (Druguet *et al.* 2014).

Current tectonic interpretations of the area ascribe the greenschist-facies shear zones, which cut the amphibolite-facies structures and granitoid bodies, to the waning stages of the Variscan orogeny, but these shear zones have never been dated. After the Variscan orogeny, several major tectonic events affected the eastern Iberian margin, which includes the Variscan rocks of the Cap de Creus peninsula. Between *c.* 170 and 140 Ma, the Piemonte–Ligurian ocean opened, breaking Adria as a promontory of Africa away from eastern Iberia (Wortmann *et al.* 2001; Vissers *et al.* 2013). Subsequent convergent motion between Iberia and Europe during the latest Cretaceous and Palaeogene led to a crustal shortening in the Pyrenees of about 150 km, accommodated by ductile and brittle thrusts emplacing Variscan blocks of the Axial Zone and northern Pyrenees in a wedge-shaped orogenic belt (Roure *et al.* 1989; Muñoz 1992; Beaumont *et al.* 2000). The Axial Zone was thus uplifted, tilted and exhumed in response to Alpine shortening. It follows that the tectonic structure of the Axial Zone may have accumulated not only Variscan but possibly also Jurassic and certainly Alpine deformations. Finally, the Oligocene and younger opening of the Gulf of Valencia affected eastern Iberia, leading to the horst and graben structure of the Catalan Coastal Range (e.g. Vergés & Fernàndez 2006).

In view of these large-scale tectonic processes during the Mesozoic and Tertiary, the interpretation of structures that postdate the climax of Variscan metamorphism is not straightforward. The lack of geochronological constraints on the age of the Cap de Creus shear zones has therefore led us to date a selection of these shear zones. Below we present an overview of the geology and new muscovite $^{40}Ar/^{39}Ar$ data, and discuss possible implications of these data for the (plate) tectonic evolution of eastern Iberia since the Variscan orogeny.

Geological setting: structure and metamorphism of the Cap de Creus peninsula

The spectacular geology of the Cap de Creus peninsula (Fig. 2) has been intensively studied by, for example, Carreras *et al.* (1977), Carreras & Casas (1987), Druguet (1997, 2001), Druguet *et al.* (1997) and Carreras (2001). The area is dominated by alternating metapsammitic and metapelitic rocks occasionally enclosing layers up to a few metres thick of light-coloured quartzite, unconformably overlain in the southeastern part of the peninsula by a siliciclastic–carbonate series. Earlier studies ascribed these siliciclastic–carbonate rocks to the Ordovician–early Devonian (Zwart (1979) or, alternatively, to the late Cambrian (see, e.g. Druguet 1997). Recently, U–Pb zircon dating (SHRIMP) of an interbedded metatuff has yielded a Cambrian age (Castiñeiras *et al.* 2008), which suggests that the entire metasedimentary sequence of the Cap de Creus peninsula has a Late Proterozoic to Cambrian age. To the south and west, granodioritic bodies of Roses and Rodes have intruded these metasediments.

The metasediments show an LP–HT field gradient over a distance of only 2 – 3 km (Figs 2 and 3), ranging from the chlorite–muscovite zone in the southern and central part of the peninsula, passing northward via the biotite zone, cordierite–andalusite zone

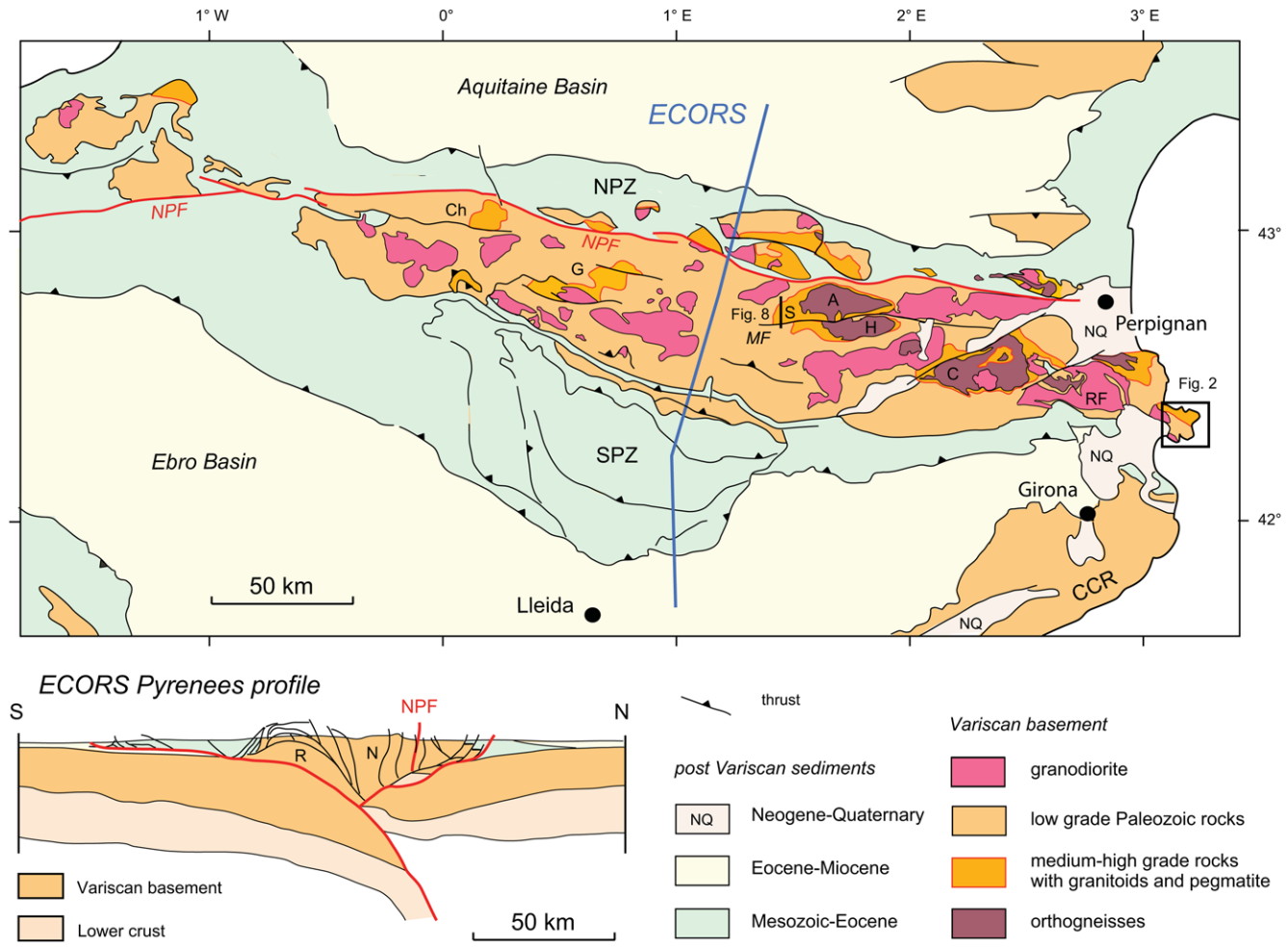

Fig. 1. Geological sketch map of the Pyrenees, compiled after Zwart (1979) and Vergés *et al.* (1995), and ECORS crustal-scale cross-section after Muñoz (1992). NPF, North Pyrenean Fault; NPZ, North Pyrenean Zone; SPZ, South Pyrenean Zone; MF, Mérens Fault; CCR, Catalan Coastal Range; A, Aston massif; H, Hospitalet massif; C, Canigou massif; Ch, Chiroulet dome; G, Garona dome; RF, Roc de Frausa massif; S, Soulcem dome. ECORS cross-section: R, Rialp unit; N, Nogueres unit; steep orientations of units south of the Rialp unit, and possible backward tilting of the Nogueres unit near the NPF, should be noted. Rectangle indicates Cap de Creus area shown in Figure 2; black line west of the Aston massif (A) denotes cross-section across the Soulcem thermal dome (S) shown in Figure 8.

and sillimanite–muscovite zone to the sillimanite–K-feldspar zone in which migmatites have locally developed (Druguet 1997; Druguet *et al.* 2014). The rocks of the sillimanite-bearing zones are extensively intruded by up to 10 m scale bodies of light-coloured pegmatite. Adjacent to the granodiorites in the south and west, the greenschist-facies metasediments are overprinted by a contact metamorphic aureole close to the intrusions (Carreras & Losantos 1982). Recent geochronological study of the migmatites and Roses granodiorite provided respectively *c*. 299 and *c*. 290 Ma U/Pb zircon ages, confirming the Variscan age of the LP–HT metamorphism and granodiorite intrusion (Druguet *et al.* 2014).

The area shows evidence of a multi-stage deformation history that is markedly heterogeneous at the scale of the peninsula (Carreras 2001). In the central, low-grade part of the peninsula, the structure is dominated by a pervasive slaty cleavage subparallel to the bedding (Fig. 4a). In the northerly amphibolite-facies rocks, the earliest structures (D_1) include occasional isoclinal folds with a penetrative axial-plane schistosity subparallel to bedding that predates the metamorphic climax (Fig. 4b). These structures are overprinted by steeply plunging second-generation folds (D_2) deforming the bedding and early schistosity (Fig. 4c and d), often with an axial-plane crenulation foliation that is commonly less pervasive than the D_1 schistosity. The D_2 structures are well developed in the amphibolite-facies rocks of the northeastern part of the peninsula, and synkinematic quartz–sillimanite aggregates indicate that D_2 affected the rocks around the metamorphic climax (Druguet *et al.* 1997; Druguet 2001). In the vicinity of the lighthouse that forms a landmark in the area (see Figs 2 and 3), and in the area immediately to the west, the axial surfaces of the D_2 folds change trend, from NE–SW at lower strains to approximately east–west at high strains to the north, delineating the margin of a complicated, steeply dipping D_2 high-strain zone within the sillimanite–K-feldspar zone between Tudela and cala Culip (Fig. 3), in which all structures are transposed to a dominant transposition foliation. A detailed structural study by Druguet *et al.* (1997) indicated that this high-strain zone results from highly vortical, sinistral non-coaxial flow with a strong component of vertical extension.

In the northern part of the peninsula, the D_1 and D_2 structures are overprinted at lower grade conditions by D_3 structures comprising spectacularly exposed, NW–SE- and east–west-trending anastomosed ductile shear zones with mylonite bands that cut across the higher-grade rocks (Fig. 4e and f). The NW–SE- and east–west-trending shear zones both have stretching lineations that moderately plunge to the NW. These shear zone structures constitute a broad shear belt, referred to by Carreras (2001) as the northern shear belt, in which a dominant set of NW–SE-trending zones have moderately to steeply dipping foliations and are dextral with an oblique reversed sense of motion, whereas the less frequent east–west-trending shear zones are commonly sinistral with an oblique normal movement sense. Detailed studies of these shear zones reveal that they may be

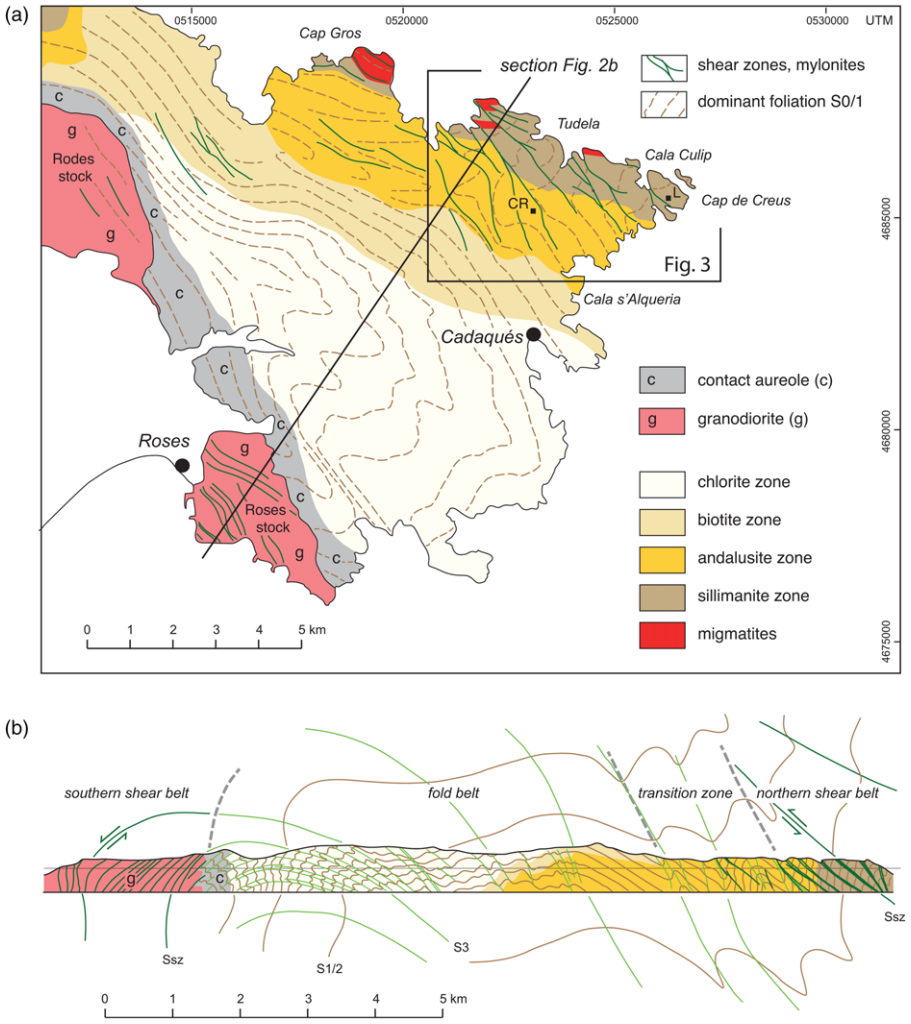

Fig. 2. (**a**) Structural sketch map of the Cap de Creus peninsula, slightly modified after Druguet *et al.* (2014). Contact metamorphic rocks adapted from 1:50000 scale geological map of Spain (Mapa Geologico de España, sheet 221, Portbou, and sheet 259, Roses). CR, Can Rabassers de Dalt; L, lighthouse. Detailed structure of the northeastern area is shown in Figure 3; black line indicates cross-section. (**b**) Structural cross-section across the Cap de Creus peninsula, after Carreras (2001).

associated with tight to isoclinal folds, which are in places clearly distinguishable from D_2 folds and are related to heterogeneous D_3 deformation affecting strongly foliated, hence anisotropic schists (Fig. 4g and h; Carreras & Casas 1987; Carreras 2001; Carreras *et al.* 2005). The D_3 structures developed under retrograde greenschist-facies conditions and are often light-coloured owing to their chlorite- and muscovite-rich compositions as opposed to the much darker biotite-rich wall rocks (Fig. 4e). Southward, the shear zones tend to vanish and are only occasionally seen in the biotite and chlorite–muscovite zones.

The heterogeneity of these structures at the scale of the peninsula (Fig. 2) led Carreras (2001) to distinguish a central fold belt dominated by a pervasive foliation subparallel to bedding and, mostly to the south, crenulation foliations that delineate a broad antiformal structure. The dominant foliation of the fold belt is commonly a low-grade slaty cleavage that is continuous with the main D_1 structure to the north, where the fold belt domain passes via a 1.5 km wide transition zone to the northern shear belt. To the south, numerous ductile shear zones in the Roses and Rodes granodiorites (Fig. 2) constitute a southern shear belt (Simpson *et al.* 1982; Carreras *et al.* 2004). At this stage we note that the heterogeneity of the large-scale structure complicates structural correlations across the peninsula as a whole. We will return to this issue in the discussion section below.

Ar–Ar geochronology

We selected three NW–SE-trending shear zones in the northern shear belt for Ar–Ar geochronology. Sample localities are shown in Figure 3. The selected shear zones include the Cala Fredosa shear zone south and west of the Cap de Creus lighthouse (locations 1 and 2, samples 13-3 and 13-9), the shear zone near Can Rabassers de Dalt (location 3, sample 14-22), and a smaller shear zone at *c.* 1.5 km NNE of Can Rabassers (location 4, sample 14-7).

With the aim of dating the micas from these shear zones, we selected samples of mica-rich bands that are illustrated in Figure 5. At the microscale, samples 13-3, 13-9 and 14-7 (Fig. 5a–c) clearly show extensional crenulations (shear bands) separating domains with relatively coarse (500 μm to 1 mm), oriented, colourless micas and confirming the sense of motion in the shear zones. The shear bands are mainly made up of dark intergrowths of very fine (10 – 50 μm) biotite and chlorite (see arrows in Fig. 5a and c), which indicate low greenschist-facies conditions during shearing. The micaceous bands in sample 14-22 (Fig. 5d), however, contain markedly fewer flakes of colourless mica, which are clearly smaller with grain sizes of 100 – 200 μm, and are surrounded by fine-grained chlorite, colourless mica and less biotite than in the shear bands of the other three samples. At higher magnifications (Fig. 5e and f), the colourless micas (arrows in Fig. 5f) are surrounded by these finer grained chlorite, colourless mica and biotite grains, suggesting a later-stage recrystallization of the precursor larger micas that are seen in the other samples (Fig. 5a–c).

Sample preparation

Whole-rock samples were crushed, ground and subsequently sieved to obtain 180 – 250 μm fractions. Muscovite separates were washed in acetone and deionized water several times and finally handpicked

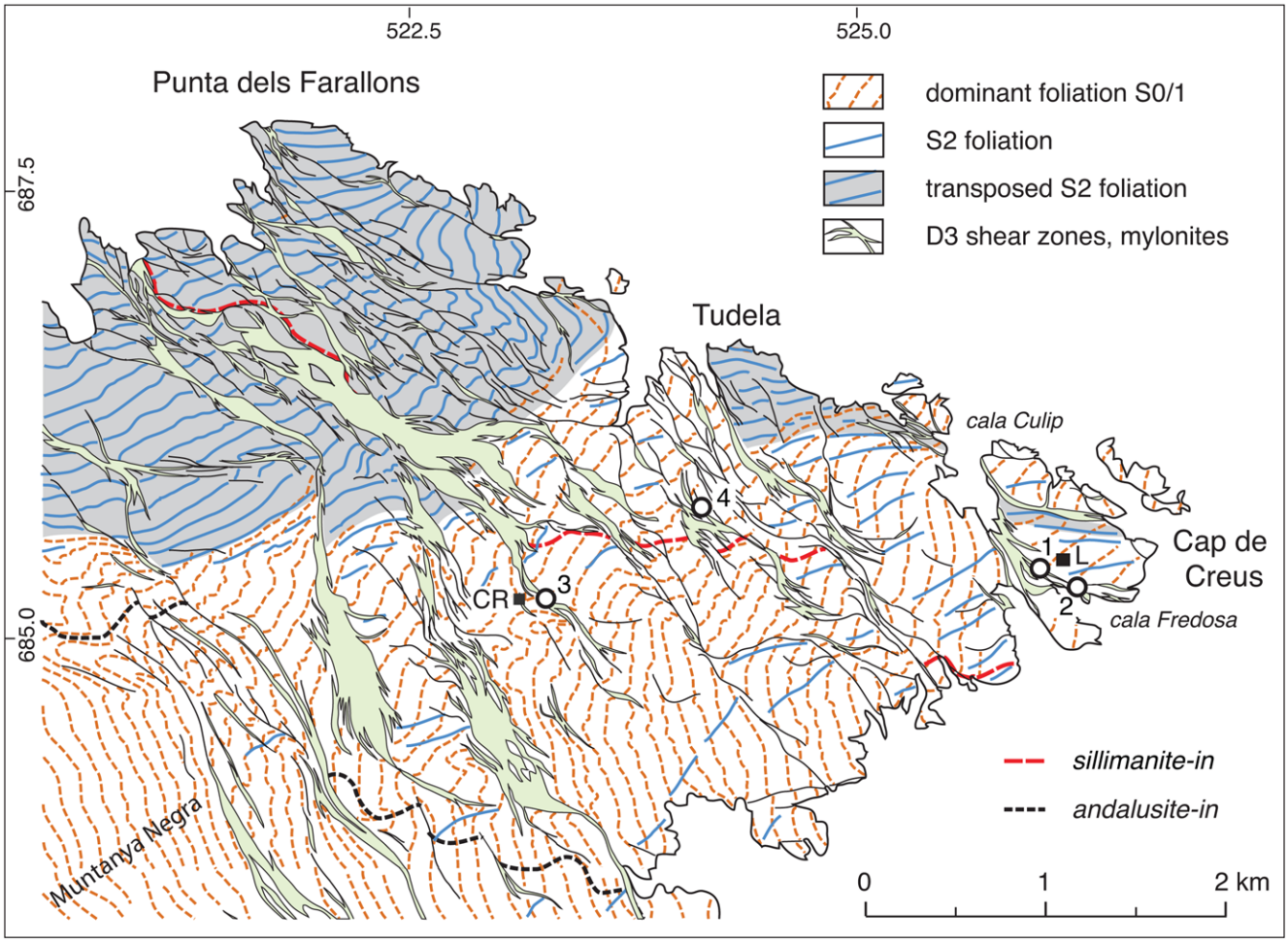

Fig. 3. Structural map of the high-grade northeastern part of the Cap de Creus peninsula, slightly modified after Druguet (2001). CR, Can Rabassers de Dalt; L, lighthouse. Andalusite-in and sillimanite-in isograds adapted from Druguet (1997). White circles labelled 1–4 denote sample localities.

under a stereomicroscope. Grains with coatings or inclusions were avoided. The separated muscovite grains were packed in aluminium capsules and irradiated in two batches together with the Taylor Creek Rhyolite (TCR) flux monitor standard and pure (zero age) K_2SO_4 and CaF_2 salts at IFE (Institutt for Energiteknikk, Kjeller, Norway) for *c.* 100 h (IFE 8) and *c.* 140 h (IFE 10), with a nominal neutron flux of 1.3×10^{13} n cm^{-2} s^{-1}. The correction factors for the production of isotopes from Ca were determined to be $(^{39}Ar/^{37}Ar)_{Ca} = (0.7907 \pm 0.00653) \times 10^{-3}$, $(^{36}Ar/^{37}Ar)_{Ca} = (3.1122 \pm 0.047) \times 10^{-4}$ and $(^{40}Ar/^{39}Ar)_K = (0.1614698 \pm 0.012631) \times 10^{-1}$ for the production of K (errors quoted at 1σ) for IFE 8, and $(^{39}Ar/^{37}Ar)_{Ca} = (3.07195 \pm 0.00784) \times 10^{-3}$, $(^{36}Ar/^{37}Ar)_{Ca} = (2.9603 \pm 0.026) \times 10^{-4}$ and $(^{40}Ar/^{39}Ar)_K = (1.3943045 \pm 0.0059335) \times 10^{-1}$ for the production of K (errors quoted at 1σ) for IFE 10.

Samples were loaded into 3.5 mm pit size aluminium sample holders and step heated using a defocused 3.5 mm CO_2 laser beam with a flat energy spectrum (Photon Machines Fusions 10.6). Extracted gases were expanded into an automated two-stage low-volume extraction line (*c.* 300 cm^3), both equipped with SAES GP-50 (st101 alloy) getters running hot (*c.* 350°C) and cold. Analyses were made using a MAP 215-50 mass spectrometer in static mode, installed at the Geological Survey of Norway. The peaks on masses $^{41-35}$Ar were determined during 10 peak hopping cycles (15 integrations per cycle, 30 integrations on mass ^{36}Ar) on a Balzers electron multiplier (SEV 217) and regressed back to zero inlet time. Following blank correction (blanks analysed every third measurement), a correction for mass fractionation, ^{37}Ar and ^{39}Ar decay and neutron-induced interference reactions produced in the reactor was undertaken using in-house software (AgeMonster written by M. Ganerød). It implements the equations of McDougall & Harrison (1999) and the newly proposed decay constant for ^{40}K after Renne *et al.* (2010). An $^{40}Ar/^{36}Ar$ ratio of 298.56 ± 0.31 from Lee *et al.* (2006) was used for the atmospheric argon correction and mass discrimination calculation (power law). We calculated J-values relative to an age of 28.619 ± 0.036 Ma for the TCR flux monitor (Renne *et al.* 2010). We define a plateau according to the following requirements: at least three consecutive steps overlapping at the 95% confidence level (1.96σ) using the strict test

$$abs(age_a - age_b) < 1.96 * \sqrt{\sigma_a^2 + \sigma_b^2}$$

(if errors quoted at 1σ) and mean square of weighted deviates (MSWD) less than the two-tailed Student *t* critical test statistics for $n - 1$. We assign dates as weighted mean plateau age (WMPA) if criteria are met and weighted mean age (WMA) if not. Weighted mean ages are calculated by weighting on the inverse of the analytical variance. If MSWD >1 the MSWD is propagated into the analytical error using the relation age ± σ × MSWD to account for this excess error contribution.

Results

Most of the analysed muscovite samples yielded highly disturbed gas release patterns; one sample produced spectra for which a WMPA (>50% of ^{39}Ar released) could be calculated, whereas the remaining three results are reported as WMA often based on spectra

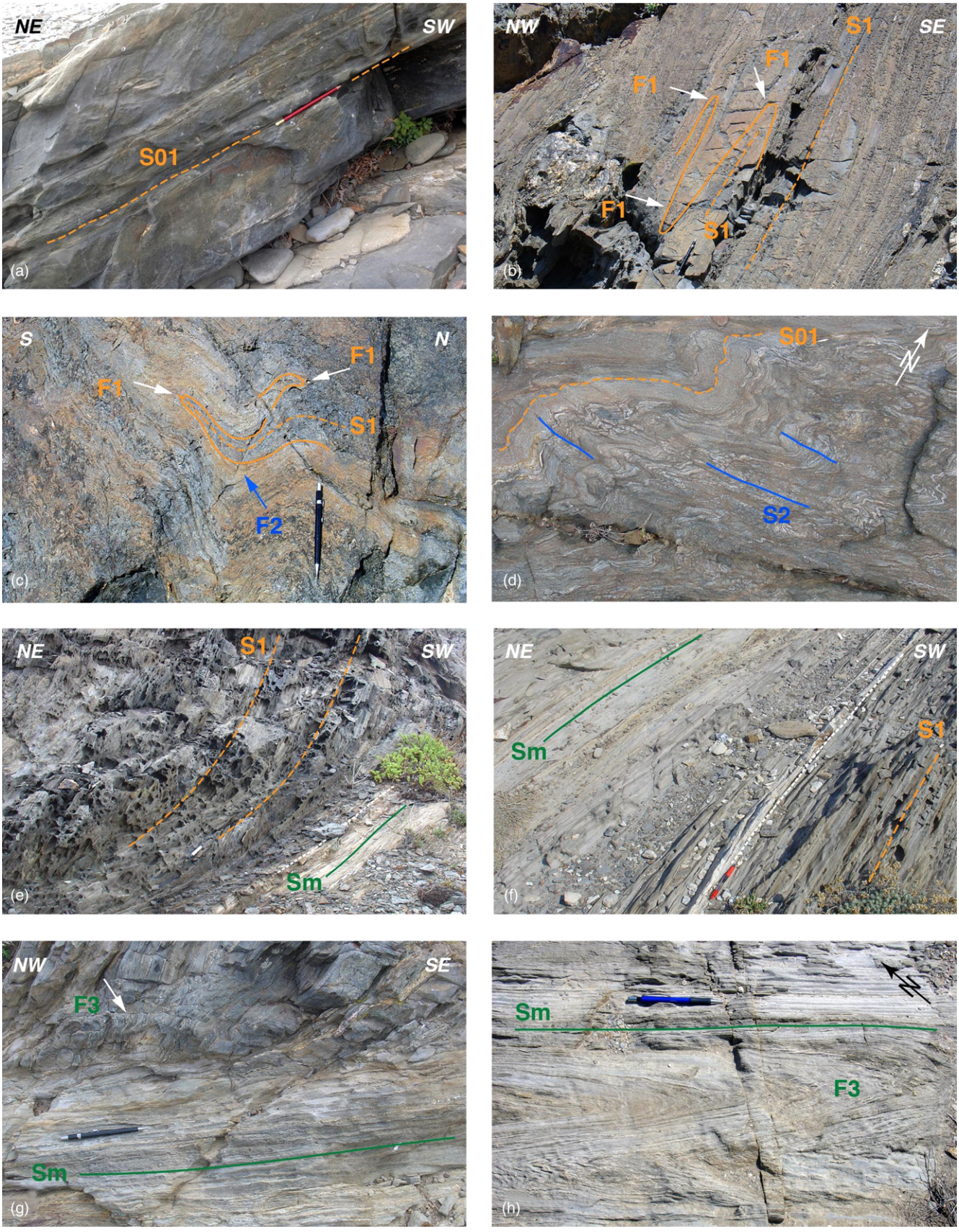

Fig. 4. Outcrop-scale deformation structures from the Cap de Creus peninsula. (**a**) Bedding transposed to main slaty cleavage ($S_{0/1}$) dipping shallowly NE, in biotite-bearing slates and phyllites at Cala s'Alqueria. (**b**) Isoclinal F_1 folds (arrows) with limbs subparallel to main foliation $S_{0/1}$ in sillimanite-zone biotite schists along road to Tudela. (**c**) Fold interference of first- and second-generation folds in sillimanite-zone schists north of the lighthouse. (**d**) Second-generation folds in sillimanite-zone schists with incipiently developed S_2 crenulation foliation in wall rock adjacent to shear zone of sample locality 4. (**e**) Gradual change of main foliation S_1 turning into the Cala Culip–Cala Fredosa shear zone at sample locality 1 west of the lighthouse. The markedly lighter colour of mylonitic rocks in the shear zone with main foliation S_m as opposed to the biotite-rich wall rock should be noted. (**f**) Aspect of the southwestern margin of the same shear zone a few metres away from (**e**). (**g**) Margin of small-scale shear zone near Tudela showing incipient F_3 folds (arrow) of earlier main structure presumably related to development of the shear zone. (**h**) Aspect of shear zone with decimetre-scale isoclinal F_3 folds embedded in strongly mylonitic core of shear zone running 200 m east of sample location 4.

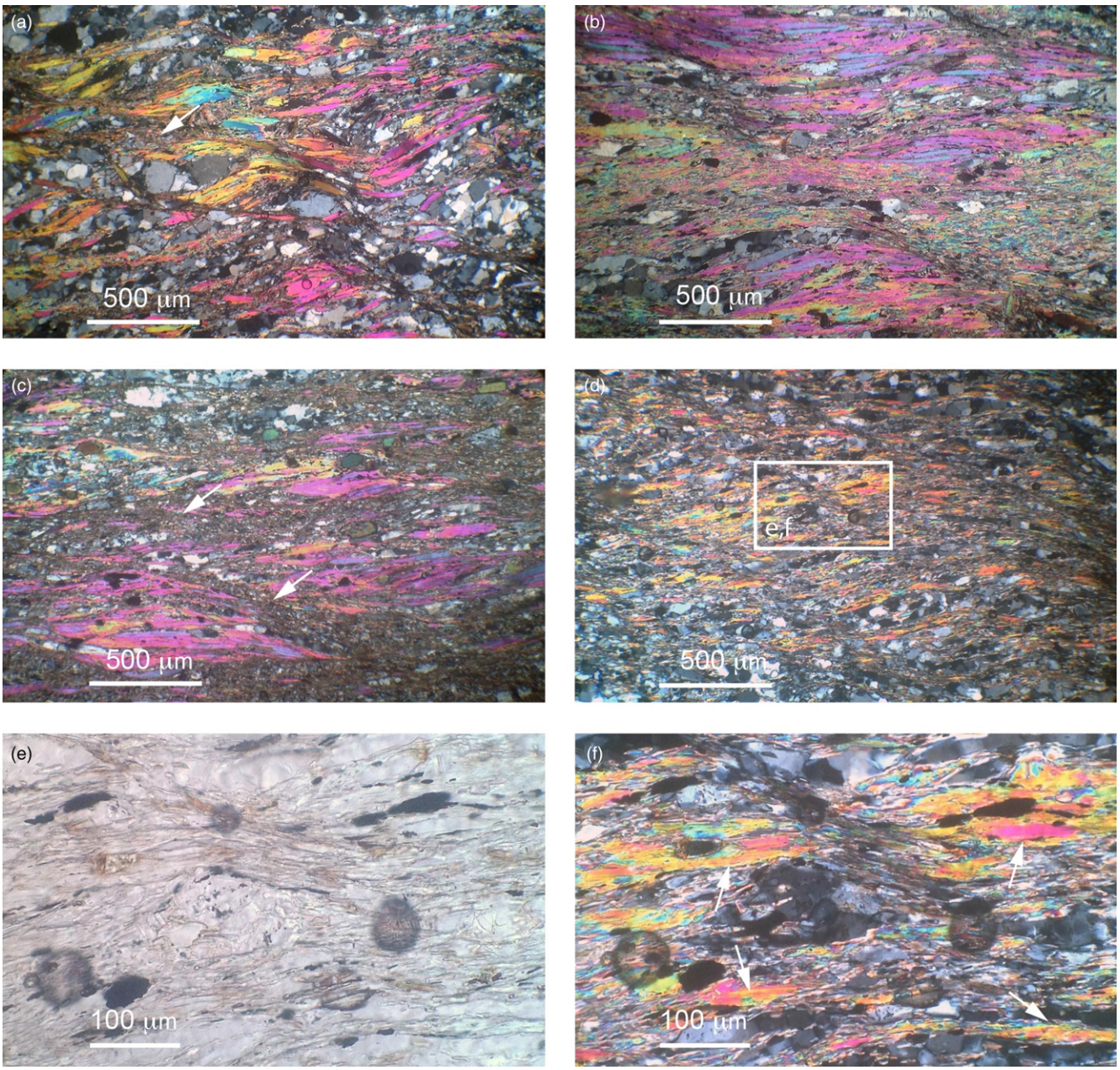

Fig. 5. Microstructures of dated shear zones. Crossed Nichols were oriented at 35° to the dominant mylonitic foliation to clearly show the micas. The wavy nature of foliation owing to small-scale shear bands (extensional crenulations) indicating dextral motion and often decorated with very fine-grained intergrowths of chlorite and biotite (arrows) should be noted. (**a**) Sample 13-3 from locality 1; (**b**) sample 13-9 from locality 2; (**c**) sample 14-7 from locality 4; (**d**) sample 14-22 from locality 3. Rectangle delineates micrographs shown in (**e**) and (**f**). (**e**) detail of (**d**), plane-polarized light. (**f**) same as (**e**), crossed Nichols; the 100 μm-scale flakes of colourless mica (arrows) surrounded by a mixture of fine-grained colourless mica, chlorite and some biotite should be noted. (For sample localities see Fig. 3.)

with a range of step ages or a total gas age (TGA). The $^{40}Ar/^{39}Ar$ age information is summarized in Table 1 and shown graphically (step-heating spectra) in Figure 6. Errors are quoted at 1.96σ level.

Muscovite separated from sample 13-3 yielded a statistically valid WMPA of 162.45 ± 0.96 Ma and a concordant inverse isochron age of 160.85 ± 4.25 Ma. Muscovite separated from sample 13-9 released *c.* 90% of the cumulative ^{39}Ar in four heating steps, and yielded two WMA of 175.18 ± 1.10 and 164.13 ± 1.24 Ma. Each WMA is based on two degassing steps and should be treated with caution; however, it should be noted that although the latter age does overlap with the WMPA of sample 13-3, we have no other reason to prefer this WMA over the other. Muscovite separated from sample 14-7 produced a highly disturbed release pattern. Therefore, the unweighted TGA of 159.23 ± 0.43 Ma better represents the bulk age of the sample. Muscovite separated from sample 14-22 yielded a WMA of 58.57 ± 0.55 Ma (39.6% cumulative ^{39}Ar).

The data presented here show variable quality; however, confidence can be placed in the Jurassic age obtained from sample 13-3. We are less confident in the data obtained from samples 13-9 and 14-7 but both samples yield a WMA that overlaps with 13-3, thus supporting a Jurassic age. Muscovite from sample 14-22 gives a Paleocene age and conforms to all criteria used to determine a WMPA except the $\%^{39}Ar$, which is <50%, and is presented here as a WMA.

To determine whether the muscovites potentially consist of mixed mica populations or recrystallized micas, we use the species $^{38}Ar_{cl}/^{39}Ar_k$ from the degassing data to plot age v. Cl/K (Fig. 7), successfully used as a discriminator in interpreting muscovite

Table 1. *$^{40}Ar/^{39}Ar$ muscovite age data (ages in Ma)*

Sample	Steps	$\%^{39}Ar$	Spectrum*	MSWD (*P*)	TGA ± 1.96σ	Isochron*	MSWD (*P*)	Intercept ± 1.96σ
13-3	3 – 6 (4)	61.12	162.45 ± 0.96	0.492 (0.688)	171.48 ± 2.08	160.85 ± 4.25	0.267 (0.000)	483.57 ± 465.90
13-9	2 – 3 (2)	72.73	175.18 ± 1.10	3.281 (0.0)	172.25 ± 0.68	n.a.	n.a.	n.a.
13-9	4 – 5 (2)	23.69	164.13 ± 1.24	0.751 (0.0)	172.25 ± 0.68	n.a.	n.a.	n.a.
14-7	1 – 15 (15)	100	160.07 ± 5.54	257.73 (0.00)	159.23 ± 0.43	125.91 ± 21.97	70.59 (0.00)	4304.26 ± 14084.72
14-22	4 – 6 (3)	39.6	58.57 ± 0.55	0.53 (0.59)	70.05 ± 0.52	57.59 ± 4.70	0.87 (0.00)	386.69 ± 392.40

MSWD, mean standard weighted deviation; TGA, total gas age; n.a., invalid inverse isochron.*Error reported as ±1.96σ.

degassing spectra from the western Alps (Villa *et al.* 2014). Samples 13-3, 13-9 and 14-7 (Fig. 7a–c) consistently show low Cl/K ratios apart from the very first degassing steps. We interpret this to probably indicate that we are degassing single muscovite populations. Sample 14-22 (Fig. 7d), however, clearly shows differences in Cl/K ratios, with higher ratios early in the step-heating experiment that clump together at low ratios containing the degassing steps used to calculated the age of the sample. This could indicate that the recrystallized rims of the muscovites formed in a tectono-metamorphic setting characterized by a more saline environment. Irrespective of the reasons for such higher saline fluid compositions, this seems well in line with the petrographic evidence mentioned above for recrystallization of the muscovites in this sample.

Analysis

The evidence for Jurassic ages of the white micas in the D_3 shear zones of the Cap de Creus northern shear belt invites us to reinterpret the tectonic significance of these structures. As shown in Figure 2b, the shear zones and associated folds have orientations close to the axial plane of a kilometre-scale folded structure in the andalusite- and sillimanite-zone rocks (Carreras 2001; Druguet 2001; Druguet *et al.* 2014), with the transposed structures and isograds in the highest grade rocks oriented vertically. The northern shear belt was suggested by Druguet (2001) and Druguet *et al.* (2014) to result from an overall transpressive tectonic regime, in which the D_3 structures developed during strike slip in the retrograde stages of the Variscan orogeny. This model presumes that, despite the post-Variscan tectonics of, for example, the Pyrenean folding and thrusting, the Cap de Creus rocks have not been significantly tilted since Variscan times. To evaluate the significance of the structural geometry at the Cap de Creus peninsula, we first review the first-order structure of the Axial Zone, to identify similarities and differences at comparable structural levels in the Variscan edifice. We then evaluate the structure of the Soulcem thermal dome in the central Pyrenees (Fig. 1), developed in essentially the same lower Palaeozoic lithology as exposed at Cap de Creus. This is followed by a

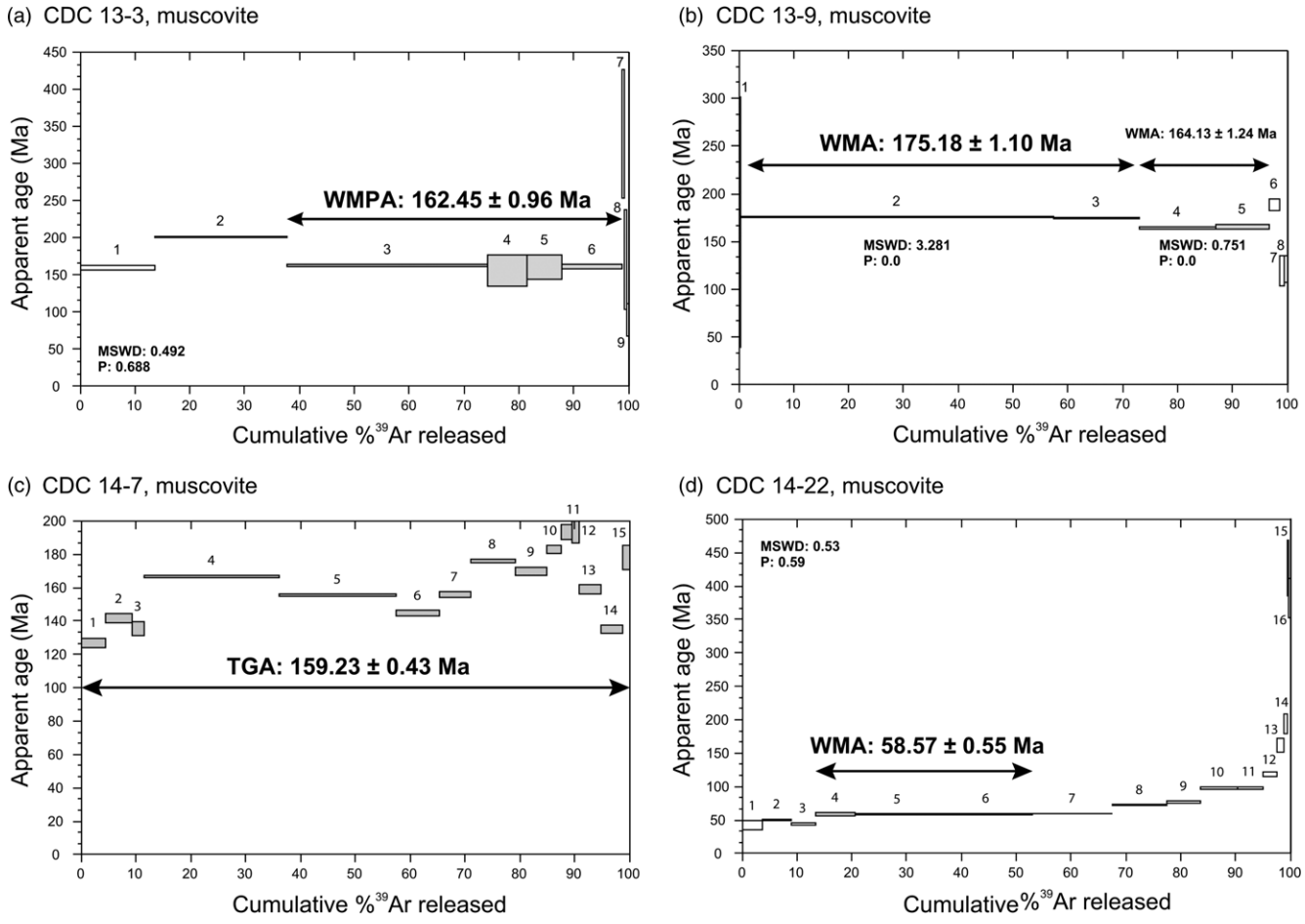

Fig. 6. $^{40}Ar/^{39}Ar$ step-heating spectra of muscovite.

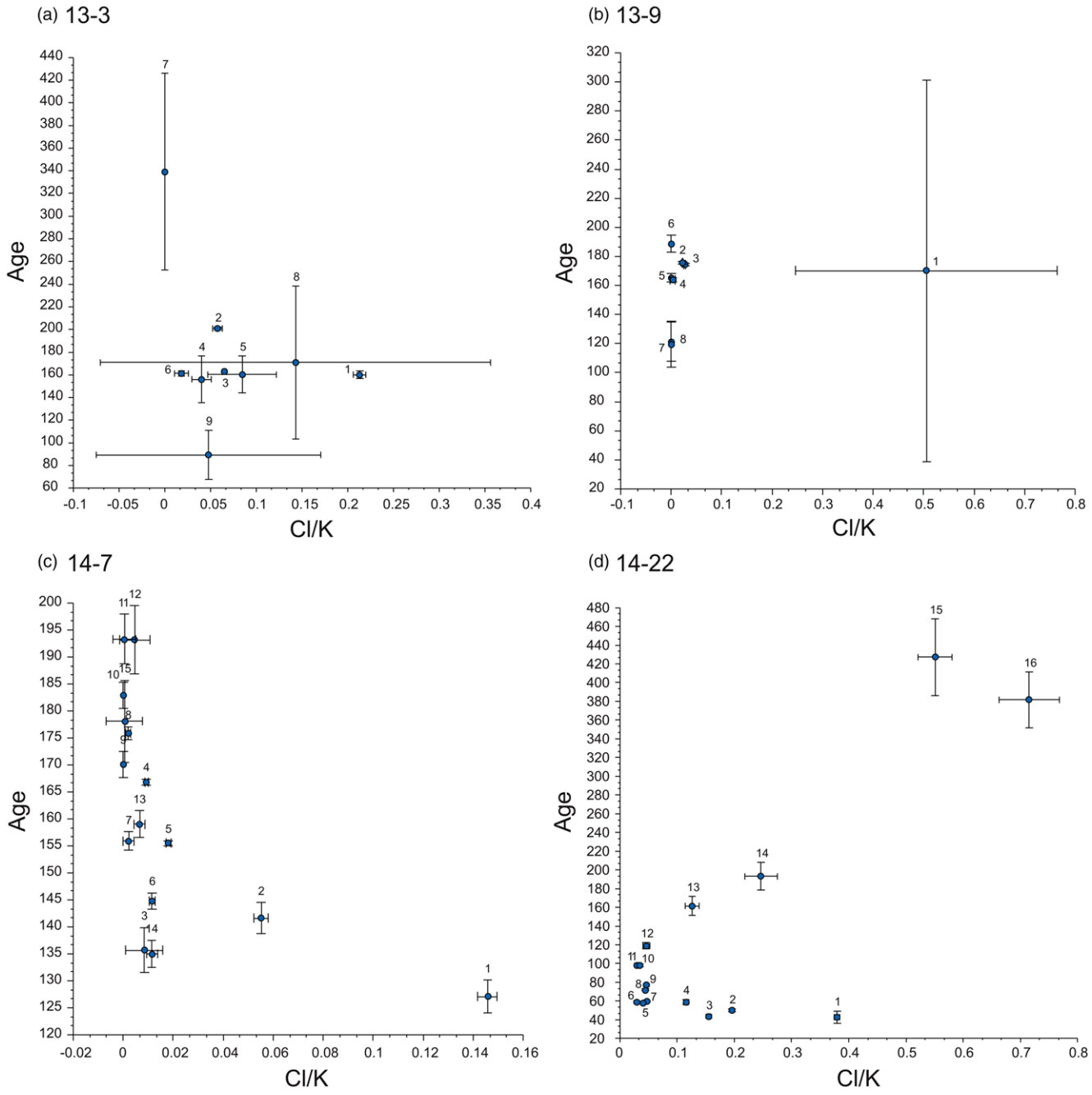

Fig. 7. Age v. Cl/K plot for the samples, calculated as $^{38}Ar_{cl}/^{39}Ar_k$. Numbers correspond to the degassing steps.

comparison of the Soulcem structure with the structure at Cap de Creus, with the aim of assessing whether the current structure of the peninsula may have been significantly tilted during Alpine orogenesis. We finally proceed to explore possible scenarios for the structural history of the Cap de Creus peninsula, and discuss their importance for understanding the plate-tectonic evolution of the western Mediterranean region.

Structural characteristics of the Axial Zone

The main structure of the Axial Zone comprises a number of domes and broad antiforms with a WNW–ESE trend and, frequently, gneissic cores bounded by Cambro-Ordovician sediments (Zwart 1979). These gneissic cores show regionally flat-lying foliations and high-grade Variscan HT–LP metamorphism. Towards the western part of the Axial Zone, the Variscan metamorphism affects higher levels of the Palaeozoic stratigraphy such as in the Garona dome in which the main amphibolite-facies foliation is also shallowly dipping to flat-lying.

De Sitter & Zwart (1960) were the first to emphasize that the dominant Variscan foliation and related folds in the Pyrenean Axial Zone show different attitudes at apparently different crustal levels. Following Wegmann (1935), they distinguished the medium- to high-grade infrastructure, characterized by a main schistosity, which formed originally with a gently dipping or flat-lying attitude, and the very low- to low-grade suprastructure dominated by steep upright folds and related foliations including slaty cleavages or very penetrative crenulation foliations. The boundary between the two structural levels may be either gradual or sharp, depending on lithology and metamorphic grade. De Sitter & Zwart (1960) suggested that the two groups of dominant structures were essentially coeval. The relationship between the gently dipping to flat-lying foliations of the metamorphic infrastructure and the steep cleavage of the low-grade suprastructure was studied by Verhoef

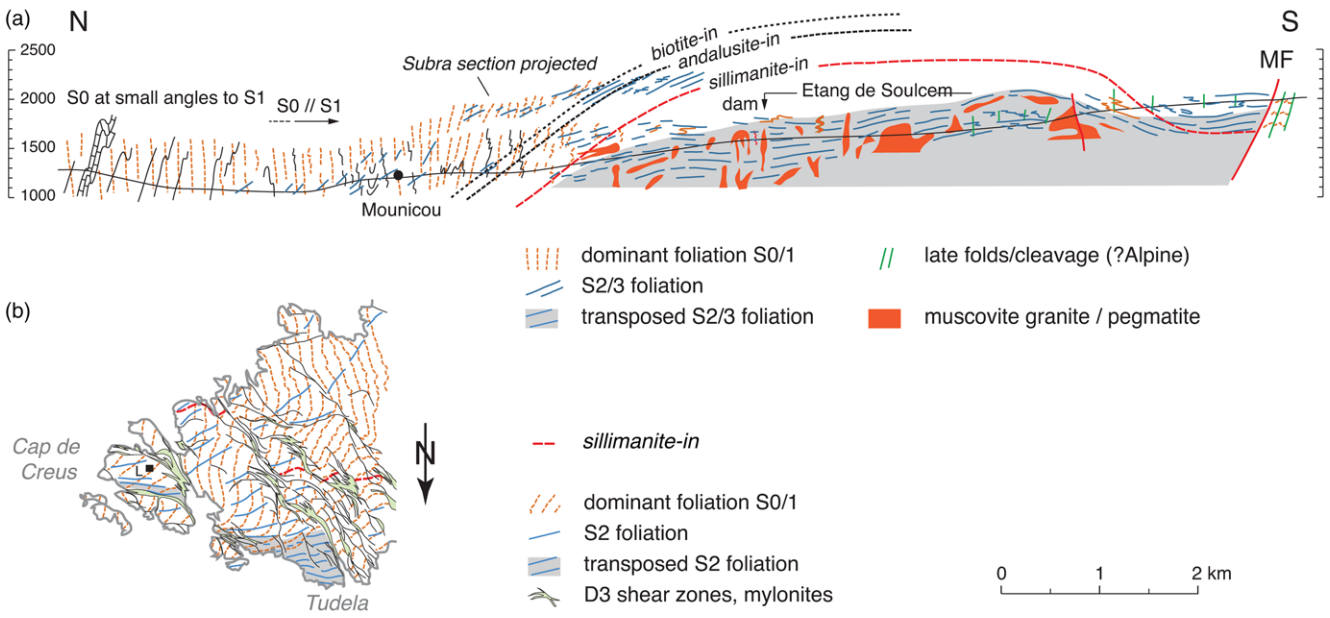

Fig. 8. (**a**) Structural cross-section across the Soulcem thermal high, modified after Verhoef *et al.* (1984), showing structural relationships between the steep suprastructure in the north and flat-lying infrastructure to the south. Section across Pla Subra, projected on this section, is located 2 km further west. (**b**) Transition at Cap de Creus from main D_1 structure to an intensely transposed D_2 structure shown in map view at same scale as (**a**), shown with north downward to facilitate comparison.

et al. (1984) around the Soulcem thermal dome at the western end of the Aston massif, and by Van den Eeckhout (1986) and Van den Eeckhout & Zwart (1988), who concluded that the flat-lying infrastructure foliations were essentially superimposed on the steeply dipping suprastructure. The associated vertical shortening led Van den Eeckhout & Zwart (1988) and Vissers (1992) to suggest an extensional tectonic setting at a late stage of the Variscan orogeny. This interpretation, however, was challenged by Carreras & Capella (1994) in a detailed discussion on the nature and significance of the suprastructure–infrastructure transition, as well as by more recent studies arguing for a transpressional tectonic setting of the Variscan belt (e.g. Evans *et al.* 1997; Gleizes *et al.* 1997, 1998; Denèle *et al.* 2009). For the present purposes we want to refrain from any large-scale interpretation in terms of tectonic regime, but instead focus on the geometry and relative timing of deformation structures. At the Cap de Creus peninsula, structures developed at variable metamorphic grade in a monotonous sequence of upper Proterozoic to Cambrian metapsammites and metapelites. The low-grade rocks of the fold belt show a simple structure dominated by a regionally flat-lying slaty cleavage, whereas to the north the structure becomes complicated by the development, at higher metamorphic grade, of D_2 structures overprinted under retrograde conditions by D_3 shear zones and associated folds. The overall structure in the high-grade domains is steep. The large-scale orientations of the main structures in the different domains are, therefore, different from the orientations of the main foliations in the supra- and infrastructure seen in the Axial Zone further west, which may suggest that the Cap de Creus rocks have been tilted relative to similar domains in the central Axial Zone.

Structure of the Soulcem dome compared with Cap de Creus

The transition between the structure of the low- and high-grade metasediments of the Cap de Creus peninsula occurs entirely within the same lithology; there is no evidence for the presence at depth of a gneissic core such as in the Canigou or Aston–Hospitalet massifs (Fig. 1), nor does the transition coincide with clearly younger stratigraphic levels as, for example, in the Garona dome (Fig. 1). The structure and metamorphism of the peninsula can perhaps best be compared with the Soulcem dome developed entirely within the Cambro-Ordovician sequence west of the Aston massif. We focus on a north–south cross-section across the Soulcem area studied in detail by Verhoef *et al.* (1984). The structure in this section (Fig. 8a) can be summarized as follows.

The northern part of the section is dominated by upright tight folds with a steeply south-dipping, penetrative axial-plane slaty cleavage and subhorizontal fold axes. Towards the south, the orientation of the S_1 cleavage changes to steeply north-dipping and the F_1 folds become isoclinal, bedding is transposed to the S_1 cleavage, and $S_{0/1}$ is overprinted by F_2 folds. The F_2 folds plunge shallowly to the west with moderately north-dipping axial planes that southward become dominant with a well-developed S_2 crenulation cleavage. In the high-grade rocks of the andalusite and sillimanite zones, occasional refolding suggests the development of a virtually horizontal S_3 foliation, but in many localities the S_2 foliations are flat-lying and pass into a transposed foliation enclosing lens-shaped domains in which relics of earlier structures are preserved. Evans *et al.* (1997) interpreted all of the flat-lying structures in the high-grade rocks of the Soulcem area as D_2 structures, and emphasized that crenulation lineations pass into stretching fabrics. Likewise, Mezger (2005) reported stretching lineations plunging at low angles towards the NW and SE. The Variscan metamorphism, represented by the ubiquitous growth of biotite, andalusite, staurolite, cordierite and sillimanite, was related by Verhoef *et al.* (1984) to the development of the flat-lying structure. In the high-grade core of the Soulcem dome, up to 10 m scale pegmatite veins and bodies of muscovite granite may be wrapped by the flat-lying foliation, or be discordant and occasionally folded, with the flat-lying transposition schistosity parallel to the axial planes.

The structural relationships seen in the Soulcem cross-section (Fig. 8a) are remarkably similar to those at the Cap de Creus peninsula seen in map view (Fig. 8b): towards the higher-grade domains, the dominant D_1 structure becomes gradually overprinted by D_2, which passes to an essentially synmetamorphic transposition foliation in the sillimanite zone (see also Fig. 3). The flat-lying transposition foliation at Soulcem shows shallowly NW- and

SE-plunging stretching lineations; that is, at moderate angles to the F_2 fold axes at higher levels. At Cap de Creus, F_2 fold axes are steep and subparallel to the stretching lineations in the high-strain zone of transposition. The main difference between the two areas is the overall orientation of the structure. At Soulcem, the early D_1 foliations are steeply oriented and the high-grade $D_{2/3}$ structure is flat-lying, whereas at Cap de Creus the low-grade D_1 structure in the fold belt is relatively flat-lying and the superimposed S_2 structure is markedly steep in the high-grade zone of intense synmetamorphic transposition. In other words, the transition between supra- and infrastructure seems tilted at Cap de Creus as compared with that at Soulcem. This raises the question of whether and to what extent each of the two areas were affected by post-Variscan tilting, and how the Variscan supra- and infrastructure were grossly oriented at the end of the Variscan orogeny. This question involves two complicating factors. First, in the southern parts of the central Axial Zone, the low-grade cleavage clearly postdates a generation of broadly NE–SW-trending pre-cleavage folds (Mey 1967; Zwart 1979). Second, as emphasized by Zwart (1979), the low-grade cleavage tends to be steep in the northern parts of the Axial Zone and gradually passes to moderately north-dipping and even subhorizontal orientations to the south such as in the Orri dome (Zwart 1979; Speksnijder 1986). This fan-shaped disposition of the main cleavage must at least in part be an Alpine feature because unconformable Triassic redbeds in Alpine thrust slices exposed in the southern part of the Axial Zone are moderately to steeply south-dipping. The Triassic redbeds are in fact the only available indicator of the late Variscan palaeo-horizontal. The angles between the redbeds and the underlying low-grade structures are generally large and vary between some 45–60° along the southern margin of the Orri dome and almost 90° further west in a section south of the Maladeta granite (Mey 1967). Where exposed, the pre-cleavage folds also have axial planes that make large angles to the Triassic unconformity. These observations suggest that the low-grade main cleavage of the suprastructure was initially rather steep. The section studied at Soulcem is located some 25 km east of the ECORS section, and the main low-grade steep slaty cleavage of the suprastructure can be traced to the northern part of the section, where all structures are equally steep and possibly less affected by tilting during Alpine thrusting than the rocks farther south. We conclude that the present-day steep suprastructure of the central Axial Zone was similarly rather steep in late Variscan times, and hence that the infrastructure foliations were flat-lying and the associated metamorphic isograds were regionally subhorizontal.

Discussion

The major antiformal structure that dominates the southern part of the Cap de Creus peninsula (Fig. 2b) comprises a northern limb of north-dipping crenulation foliations that pass via a flat-lying hinge domain into the south-dipping shear zones of the southern shear belt. The apparent continuity, across the granite intrusive contact, of the crenulation foliations with the shear zones in the granite was first reported by Carreras & Losantos (1982). Those researchers also showed that the crenulation foliation postdates the contact metamorphism of the metapelites. Carreras (2001) suggested that the crenulation foliation in the south can be correlated with the D_3 structures in the north and consequently indicated this foliation as S_3 (Fig. 2b). This relative dating of the crenulation foliation in the south is consistent with recent dating of the Roses granite (290.8 ± 2.9 Ma; Druguet *et al.* 2014) as follows. The crenulation foliation in the south postdates the contact metamorphism, and hence must be younger than the granite. The synmetamorphic D_2 crenulation foliations in the high-grade rocks in the north are associated with syntectonic partial melts dated at 298.8 ± 3.8 Ma (Druguet *et al.* 2014). Consequently, the crenulation foliation in the south must be at least some 10 myr younger than the synmetamorphic D_2 crenulation foliations in the north, but may well correspond to third-generation folds associated with the shear zones of the northern shear belt (Carreras & Casas 1987; Carreras 2001).

The large-scale antiform adjacent to the Roses granite was interpreted by Carreras (2001) as the result of Alpine overturning similar to the steep southward tilts seen in the southern Axial Zone of the central Pyrenees and well studied in the ECORS crustal section (Fig. 1). Carreras (2001) has suggested that such Alpine overturning may explain the dominantly sinistral shear senses in the southern shear belt as opposed to the dominantly dextral motions in the north.

There are no Triassic or younger Mesozoic rocks exposed at Cap de Creus to convincingly demonstrate any Alpine tilting. As outlined above, the central and northern parts of the peninsula are characterized by a regionally gently dipping to flat-lying, low-grade slaty cleavage occasionally overprinted by crenulations, and passing northwards to a complicated large-scale fold structure in which D_1 and D_2 structures are overprinted by the D_3 structures of the northern shear belt. The large-scale structure was interpreted by Druguet (2001) as being due to D_2 steepening of the high-grade domain in a transpressional tectonic regime that progressively evolved during Variscan retrogression with the development of the northern shear belt. Our age data from a few of these shear zones, however, cast doubt on the progressive nature of the D_2 and D_3 deformations, and invite us to explore alternatives.

A possible scenario for the structural history at Cap de Creus

Although we agree with the notion of possible Alpine overturning in the southern part of the peninsula, we perceive no fundamental argument to preclude similar large-scale Alpine tilting in the north. Such Alpine tilting would explain why the suprastructure–infrastructure transition and dominant D_2 transposition foliation and associated isograds are steep, as opposed to the generally flat-lying infrastructure in the central Axial Zone. To explore the consequences of such tilting we perform a thought experiment illustrated in Figure 9 in which the mean orientations of the structures in the high-grade domain (Fig. 9a) reported by Druguet *et al.* (1997) and Carreras (2001) are backrotated about a horizontal tilt axis trending WNW (290°/0°) (i.e. parallel to the strike of the steeply dipping isograds) over an angle of 90° that brings the infra- and suprastructure into similar orientations as observed in the Soulcem dome. It should be noted that a horizontal tilt axis parallel to the strike of the isograds ensures that the isograd surfaces become subhorizontal after rotation. The result is shown in Figure 9b. The rotation changes the steep structures into moderately dipping ones, with the $S_{0/1}$ steeper than the S_2 foliations and the D_2 stretching direction subhorizontal trending NE–SW. The NW–SE-trending reverse dextral shear zones after rotation become moderately WSW-dipping, with downdip stretching directions (i.e. they would become ductile normal faults). The east–west-trending sinistral shears become rotated to shallowly south-dipping oblique reverse shears, also with WSW-plunging stretching lineations. Together with the backrotated NW–SE-trending shears they form a conjugate set suggesting subhorizontal ENE–WSW-directed stretching and subvertical shortening.

The 175 – 160 Ma Jurassic ages obtained from the Cap de Creus shear zones, combined with their location in the easternmost part of Iberia, suggest that these structures are related to the coeval rifting history of the Piemonte–Ligurian ocean separating Adria from Iberia. A kinematic model based on marine magnetic anomalies of the Atlantic Ocean shows that the Piemonte–Ligurian opened by NNE–SSW-directed extension in the Piemonte–Ligurian domain between the Black Spur Magnetic Anomaly (*c.* 170 Ma) and anomaly M21 (*c.* 149.5 Ma) (Vissers *et al.* 2013). The averaged

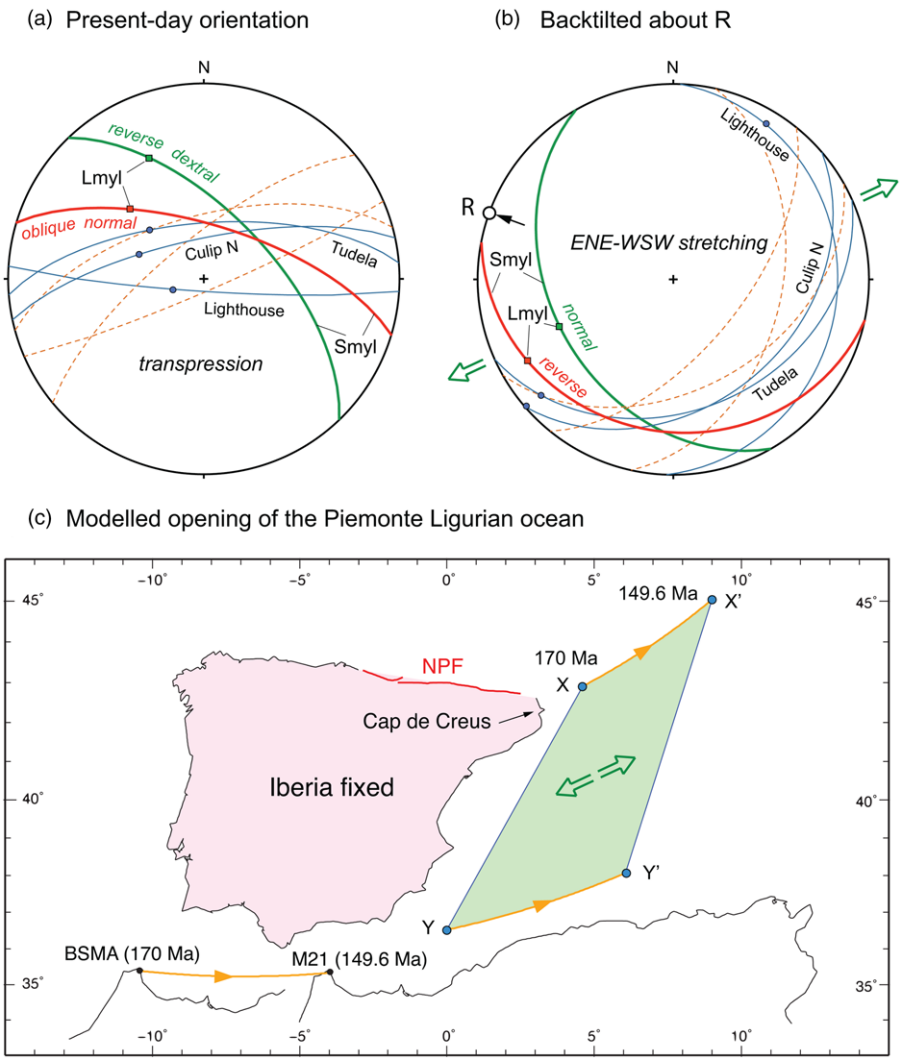

Fig. 9. (**a**) Mean orientations of NW–SE-trending dextral shear zones and east–west-trending sinistral shear zones in the northern shear belt, from Carreras (2001), and mean steeply oriented S_1 (thin dashed lines) and S_2 foliations (thin solid lines) reported by Druguet *et al.* (1997) for the Tudela, Lighthouse and norther Culip subareas. Smyl, mylonitic foliation; Lmyl, stretching lineation. These structures and their orientations were interpreted by Druguet (2001) as a result of bulk transpression during the Variscan orogeny. (**b**) Orientations of structures shown in (**a**) after 90° rotation about a NNW–SSE-trending axis (290°–0°). The moderately dipping S_1 (thin dashed lines), shallowly dipping S_2 (thin solid lines), and subhorizontal stretching lineations on S_2 should be noted. The NW–SE-trending reverse dextral shear zones after rotation become ductile normal shears with a mean dip to the WSW and dip-slip stretching lineations, consistent with roughly ENE–WSW-directed extension. The east–west-trending sinistral shear zones become shallowly dipping oblique reverse shears, also with ENE–WSW-directed stretching lineations. (**c**) Modelled opening of the Piemonte–Ligurian basin shown with respect to Iberia in its present-day orientation, after Vissers *et al.* (2013). X and Y denote arbitrarily chosen marker points on the rift zone developing between Adria and Iberia since the Middle Jurassic. Ages of magnetic anomalies in the central Atlantic Ocean: BSMA (Black Spur Magnetic Anomaly), 170 Ma; M21, 149.57 Ma. Modelled bulk extension direction in the Piemonte–Ligurian domain is about WSW–ENE; that is, in good agreement with the stretching direction inferred from the Cap de Creus shear zones after rotation.

relative motion of Adria with respect to Iberia during that time span, shown in its present-day orientation, is ENE–WSW (Fig. 9c). It follows that the shear zones of the northern shear belt in their backrotated orientation fit remarkably well with the extension direction modelled for rifting and drifting in the Piemonte–Ligurian basin. At the same time, the inferred reverse transpressive kinematics of the shear zones as implied by their present-day orientation seems inconsistent with Jurassic extension during the Piemonte–Ligurian break-up.

Our analysis of the structure at Cap de Creus assumes the possibility of large-scale Alpine rotations about subhorizontal axes, presumably owing to the development of a thrust structure at depth analogous to the Alpine structure along the ECORS seismic section in the central Pyrenees. Large tracts of Variscan basement in the Axial Zone show limited or no evidence for Alpine imprint at the outcrop scale, and seem to be affected by only localized deformation along thrust contacts and rotations about subhorizontal axes caused by the development of the Alpine thrust stack. Such rotations, however, may have affected significant portions of the Axial Zone and hence the spatial arrangement of the suprastructure–infrastructure geometry. The presence of Mesozoic rocks in the central Axial Zone and the ECORS study and associated drillholes facilitate this interpretation, but at Cap de Creus no Mesozoic rocks are present to differentiate between Variscan and Alpine structure, and north of the steep high-grade sediments the Variscan basement is covered by a marine Neogene basin. It is therefore impossible to conclusively establish the initial orientation of the Variscan structure on the Cap de Creus peninsula. Our suggestion that this structure was tilted must be therefore be viewed as a viable hypothesis. Alpine tilting accounts for the shallow-dipping arrangement of the suprastructure–infrastructure geometry, which is much steeper in the central Axial Zone, and for the steep orientation of the isograds in the north, and the dextral reverse shear zones yielding Jurassic ages would be tilted ductile normal faults representing pre-drift continental extension related to the opening of the Piemonte–Ligurian ocean. Although the steep orientation of the D_2 high-strain zone is currently interpreted in terms of a Variscan transpressional tectonic regime, we do not reject this tectonic setting for the Pyrenean Variscan belt but we prefer to interpret the structural geometry at Cap de Creus in terms of a Variscan D_1/D_2 and associated HT–LP metamorphism, Jurassic stretching and development of the D_3 shear zone structures, followed by Alpine tilting and thrust stacking at depth during the Tertiary. The Alpine age (58.57 ± 0.55 Ma) recorded in the shear zone at location 4 (sample 14-22) could represent either reactivation of a Jurassic shear zone or a newly formed Alpine shear zone developed in its present-day orientation. We thus suggest that the structure of the Cap de Creus peninsula reflects multi-stage deformation. If our interpretation is correct, then Cap de Creus could be an exposed equivalent of a continental passive margin that underwent ductile stretching during (ultra-)slow spreading, and may

be equivalent to structures now buried below the west Iberian or Newfoundland margin.

Conclusion

The existing lack of geochronological constraints on the age of the greenschist-facies ductile shear zones exposed on the Cap de Creus peninsula has led us to date a few of these shear zones. $^{40}Ar/^{39}Ar$ dating of white micas from selected shear zones at Cap de Creus yields Jurassic ages including a robust result of 162.45 ± 0.96 Ma, supported by weighted mean ages of 175.18 ± 1.10 and 164.13 ± 1.24 Ma and a total gas age of 159.33 ± 0.43 Ma, and one Tertiary (58.57 ± 0.55 Ma) age. This contradicts the current structural studies of the area, which assume that the shear zones developed during the retrograde stages of the Variscan orogeny. We suggest that the present-day structure at Cap de Creus resulted from Variscan progressive D_1 and D_2 deformation and allied HT–LP metamorphism, followed by crustal stretching during the Jurassic and development of ductile normal faults reflecting pre-drift continental extension related to opening of the Piemonte–Ligurian basin. Alpine tilting during the Tertiary caused steepening in much of the northern part of the area into a steep attitude and the ductile normal faults became rotated to their present orientations as dextral reverse shear zones. The shear zone yielding a Tertiary age could reflect either an Alpine structure or reactivation of an earlier, presumably Jurassic shear zone.

Acknowledgements and Funding

D.J.J.v.H. acknowledges funding through ERC Starting Grant 306810 (SINK) and NWO VIDI grant 864.11.004. We are indebted to an anonymous reviewer and to editor I. M. Villa for helpful questions and suggestions that greatly improved the paper.

Scientific editing by Igor Villa

References

Beaumont, C., Muñoz, J.A., Hamilton, J. & Fullsack, P. 2000. Factors controlling the alpine evolution of the central Pyrenees inferred from a comparison of observations and geodynamical models. *Journal of Geophysical Research*, **105**, 8121–8145.

Carreras, J. 2001. Zooming on Northern Cap de Creus shear zones. *Journal of Structural Geology*, **23**, 1457–1486.

Carreras, J. & Capella, J. 1994. Tectonic levels in the Paleozoic basement of the Pyrenees: a review and a new interpretation. *Journal of Structural Geology*, **16**, 1509–1524.

Carreras, J. & Casas, J.M. 1987. On folding and shear zone development: a mesoscale structural study on the transition between two different tectonic styles. *Tectonophysics*, **135**, 87–98.

Carreras, J. & Losantos, M. 1982. Geological setting of the Roses granodiorite (E-Pyrenees, Spain). *Acta Geológica Hispánica*, **17**, 219–225.

Carreras, J. & Santanach, P. 1973. Micropliegues y movimiento en los cizallamientos profundos del cabo de Creus (prov. Gerona). *Estudios Geológicos*, **29**, 439–450.

Carreras, J., Estrada, A. & White, S. 1977. The effects of folding on the *c*-axis fabrics of a quartz-mylonite. *Tectonophysics*, **39**, 3–24.

Carreras, J., Druguet, E., Griera, A. & Soldevila, J. 2004. Strain and deformation history in a syntectonic pluton. The case of the Roses granodiorite (Cap de Creus, Eastern Pyrenees). *In*: Alsop, G.I., Holdsworth, R.E., McCaffrey, K.J.W. & Hand, W. (eds) *Flow Processes in Faults and Shear Zones*. Geological Society, London, Special Publications, **224**, 307–319, http://doi.org/10.1144/GSL.SP.2004.224.01.19

Carreras, J., Druguet, E. & Griera, A. 2005. Shear zone-related folds. *Journal of Structural Geology*, **27**, 1229–1251, http://doi.org/10.1016/j.jsg.2004.08.004

Castiñeiras, P., Navidad, M., Liesa, M., Carreras, J. & Casas, J.M. 2008. U–Pb zircon ages (SHRIMP) for Cadomian and Early Ordovician magmatism in the Eastern Pyrenees: New insights into the pre-Variscan evolution of the northern Gondwana margin. *Tectonophysics*, **461**, 228–239, http://doi.org/10.1016/j.tecto.2008.04.005

Denèle, Y., Olivier, P., Gleizes, G. & Barbey, P. 2009. Decoupling between the middle and upper crust during transpression-related lateral flow: Variscan evolution of the Aston gneiss dome (Pyrenees, France). *Tectonophysics*, **477**, 244–261.

De Sitter, L.U. & Zwart, H.J. 1960. Tectonic development in supra- and infra-structures of a mountain chain. *In*: Kale, A. & Metzler, A. (eds) *Structure of the Earth's crust and deformation of rocks, Proceedings 21st International Geological Congress*. Det Berlingske Bogtrykkeri, Copenhagen, **18**, 248–256.

Druguet, E. 1997. *The structure of the NE Cap de Creus peninsula. Relationships with metamorphism and magmatism*. PhD thesis, Universitat Autònoma de Barcelona.

Druguet, E. 2001. Development of high thermal gradients by coeval transpression and magmatism during the Variscan orogeny: insights from the Cap de Creus (Eastern Pyrenees). *Tectonophysics*, **332**, 275–293.

Druguet, E., Passchier, C.W., Carreras, J., Victor, P. & den Brok, S. 1997. Analysis of a complex high-strain zone at Cap de Creus, Spain. *Tectonophysics*, **280**, 31–45.

Druguet, E., Castro, A., Chichorro, M., Francisco Pereira, M. & Fernández, C. 2014. Zircon geochronology of intrusive rocks from Cap de Creus, Eastern Pyrenees. *Geological Magazine*, **151**, 1095–1114, http://doi.org/10.1017/S0016756814000041

Evans, N.G., Gleizes, G., Leblanc, D. & Bouchez, J.L. 1997. Hercynian tectonics in the Pyrenees: a new view based on structural observations around the Bassiès granite pluton. *Journal of Structural Geology*, **19**, 195–208, http://doi.org/10.1016/S0191-8141(96)00080-6

Gleizes, G., Leblanc, D. & Bouchez, J.L. 1997. Variscan granites of the Pyrenees revisited: their role as syntectonic markers of the orogen. *Terra Nova*, **9**, 38–41.

Gleizes, G., Leblanc, D. & Bouchez, J.L. 1998. The main phase of the Hercynian orogeny of the Pyrenees is a dextral transpression. *In*: Holdsworth, R.E., Stracham, R.A. & Dewey, J.F. (eds) *Continental Transpressional and Transtensional Tectonics*. Geological Society, London, Special Publications, **135**, 267–273, http://doi.org/10.1144/GSL.SP.1998.135.01.17

Lee, J.Y., Marti, K., Severinghaus, J.P., Kawamura, K., Yoo, H.S., Lee, J.B. & Kim, J.S. 2006. A redetermination of the isotopic abundances of atmospheric Ar. *Geochimica et Cosmochimica Acta*, **70**, 4507–4512.

McDougall, I. & Harrison, T.M. 1999. *Geochronology and thermochronology by the $^{40}Ar/^{39}Ar$ method*. Oxford University Press, New York.

Mey, P.H.W. 1967. The geology of the Upper Ribagorzana and Baliera valleys, Central Pyrenees, Spain. *Leidse Geologische Mededelingen*, **41**, 153–220.

Mezger, J.E. 2005. Comparison of the western Aston–Hospitalet and the Bossòst domes: evidence for polymetamorphism and its implications for the Variscan tectonic evolution of the Axial Zone of the Pyrenees. *Journal of the Virtual Explorer*, **19**, paper 6, http://doi.org/10.3809/jvirtex.2005.00122

Muñoz, J.A. 1992. Evolution of a continental collision belt: ECORS-Pyrenees crustal balanced cross-section. *In*: McClay, K.R. (ed.) *Thrust Tectonics*. Chapman & Hall, London, 235–246.

Renne, P.R., Mundil, R., Balco, G., Min, K.W. & Ludwig, K.R. 2010. Joint determination of ^{40}K decay constants and $^{40}Ar^*/^{40}K$ for the Fish Canyon sanidine standard, and improved accuracy for $^{40}Ar/^{39}Ar$ geochronology. *Geochimica et Cosmochimica Acta*, **74**, 5349–5367.

Roure, F., Choukroune, P. *et al.* 1989. ECORS deep seismic data and balanced cross-sections: geometric constraints on the evolution of the Pyrenees. *Tectonics*, **8**, 41–50.

Simpson, C., Carreras, J. & Losantos, M. 1982. Inhomogeneous deformation in Roses granodiorite. *Acta Geológica Hispánica*, **17**, 219–226.

Speksnijder, A. 1986. Geological analysis of Paleozoic large-scale faulting in the south–central Pyreees. *Geologica Ultraiectina*, **43**, 1–211.

Van den Eeckhout, B. 1986. A case study of a mantled gneiss antiform, the Hospitalet massif, Pyrenees (Andorre, France). *Geologica Ultraiectina*, **45**, 1–193.

Van den Eeckhout, B. & Zwart, H.J. 1988. Hercynian crustal-scale extensional shear zone in the Pyrenees. *Geology*, **16**, 135–138.

Vergés, J. & Fernàndez, M. 2006. Ranges and basins in the Iberian Peninsula: their contribution to the present topography. *In*: Gee, D.G. & Stephenson, R.A. (eds) *European Lithosphere Dynamics*. Geological Society, London, Memoirs, **32**, 223–234, http://doi.org/10.1144/GSL.MEM.2006.032.01.13

Vergés, J., Millan, H. *et al.* 1995. Eastern Pyrenees and related foreland basins: pre-, syn- and post-collisional crustal-scale cross-sections. *Marine and Petroleum Geology*, **12**, 903–916.

Verhoef, P.N.W., Vissers, R.L.M. & Zwart, H.J. 1984. A new interpretation of the structural and metamorphic history of the western Aston massif (Central Pyrenees, France). *Geologie en Mijnbouw*, **63**, 399–410.

Villa, I.M., Bucher, S., Bousquet, R., Kleinhanns, I.C. & Schmid, S.M. 2014. Dating polygenetic metamorphic assemblages along a transect across the Western Alps. *Journal of Petrology*, **55**, 803–830, http://doi.org/10.1093/petrology/egu007

Vissers, R.L.M. 1992. Variscan extension in the Pyrenees. *Tectonics*, **11**, 1369–1384.

Vissers, R.L.M., van Hinsbergen, D.J.J., Meijer, P.Th. & Piccardo, G.B. 2013. Kinematics of Jurassic ultra-slow spreading in the Piemonte Ligurian ocean. *Earth and Planetary Science Letters*, **380**, 138–150.

Wegmann, C.E. 1935. Zur Deutung der Migmatite. *Geologische Rundschau*, **26**, 305–350.

Wortmann, U.G., Weissert, H., Funk, H. & Hauck, J. 2001. Alpine plate kinematics revisited: The Adria Problem. *Tectonics*, **20**, 134–147.

Zwart, H.J. 1979. The geology of the central Pyrenees. *Leidse Geologische Mededelingen*, **50**, 1–74.